Measurements of Branching Fractions for $B \to K\pi$ and $B \to \pi\pi$ Decays

S.-W. Lin,[25] P. Chang,[25] K. Abe,[9] K. Abe,[43] I. Adachi,[9] H. Aihara,[45] D. Anipko,[1] V. Aulchenko,[1] T. Aushev,[17,13] S. Bahinipati,[3] A. M. Bakich,[41] E. Barberio,[20] I. Bedny,[1] U. Bitenc,[14] I. Bizjak,[14] S. Blyth,[23] A. Bondar,[1] A. Bozek,[26] M. Bračko,[9,19,14] T. E. Browder,[8] M.-C. Chang,[4] Y. Chao,[25] A. Chen,[23] K.-F. Chen,[25] W. T. Chen,[23] B. G. Cheon,[7] R. Chistov,[13] S.-K. Choi,[6] Y. Choi,[40] Y. K. Choi,[40] J. Dalseno,[20] M. Dash,[49] J. Dragic,[9] A. Drutskoy,[3] S. Eidelman,[1] S. Fratina,[14] N. Gabyshev,[1] A. Garmash,[34] A. Go,[23] B. Golob,[18,14] H. Ha,[16] J. Haba,[9] T. Hara,[31] H. Hayashii,[22] M. Hazumi,[9] D. Heffernan,[31] T. Hokuue,[21] Y. Hoshi,[43] W.-S. Hou,[25] Y. B. Hsiung,[25] T. Iijima,[21] K. Ikado,[21] A. Imoto,[22] K. Inami,[21] A. Ishikawa,[45] H. Ishino,[46] R. Itoh,[9] M. Iwasaki,[45] Y. Iwasaki,[9] H. Kaji,[21] P. Kapusta,[26] S. U. Kataoka,[22] H. Kawai,[2] T. Kawasaki,[28] H. Kichimi,[9] Y. J. Kim,[5] K. Kinoshita,[3] S. Korpar,[19,14] P. Križan,[18,14] P. Krokovny,[9] R. Kulasiri,[3] R. Kumar,[32] A. Kuzmin,[1] Y.-J. Kwon,[50] M. J. Lee,[38] T. Lesiak,[26] D. Liventsev,[13] J. MacNaughton,[11] F. Mandl,[11] T. Matsumoto,[47] S. McOnie,[41] T. Medvedeva,[13] W. Mitaroff,[11] H. Miyake,[31] H. Miyata,[28] Y. Miyazaki,[21] G. R. Moloney,[51] E. Nakano,[30] M. Nakao,[9] H. Nakazawa,[23] Z. Natkaniec,[26] S. Nishida,[9] O. Nitoh,[48] S. Ogawa,[42] T. Ohshima,[21] S. Okuno,[15] S. L. Olsen,[8] Y. Onuki,[35] H. Ozaki,[9] P. Pakhlov,[13] G. Pakhlova,[13] C. W. Park,[40] R. Pestotnik,[14] L. E. Piilonen,[49] H. Sahoo,[8] Y. Sakai,[9] N. Satoyama,[39] T. Schietinger,[17] O. Schneider,[17] J. Schümann,[9] A. J. Schwartz,[3] K. Senyo,[21] M. E. Sevior,[20] M. Shapkin,[12] H. Shibuya,[42] B. Shwartz,[1] J. B. Singh,[32] A. Somov,[3] N. Soni,[32] S. Stanič,[29] M. Starič,[14] H. Stoeck,[41] K. Sumisawa,[9] T. Sumiyoshi,[47] S. Suzuki,[36] S. Y. Suzuki,[9] F. Takasaki,[9] K. Tamai,[9] M. Tanaka,[9] G. N. Taylor,[20] Y. Teramoto,[30] X. C. Tian,[33] I. Tikhomirov,[13] T. Tsukamoto,[9] S. Uehara,[9] K. Ueno,[25] Y. Unno,[7] S. Uno,[9] Y. Ushiroda,[9] G. Varner,[8] K. E. Varvell,[41] S. Villa,[17] C. C. Wang,[25] C. H. Wang,[24] M.-Z. Wang,[25] Y. Watanabe,[46] J. Wicht,[17] E. Won,[16] Q. L. Xie,[10] B. D. Yabsley,[41] A. Yamaguchi,[44] Y. Yamashita,[27] M. Yamauchi,[9] Y. Yusa,[49] C. C. Zhang,[10] Z. P. Zhang,[37] and A. Zupanc[14]

(Belle Collaboration)

[1]*Budker Institute of Nuclear Physics, Novosibirsk*
[2]*Chiba University, Chiba*
[3]*University of Cincinnati, Cincinnati, Ohio 45221*
[4]*Department of Physics, Fu Jen Catholic University, Taipei*
[5]*The Graduate University for Advanced Studies, Hayama*
[6]*Gyeongsang National University, Chinju*
[7]*Hanyang University, Seoul*
[8]*University of Hawaii, Honolulu, Hawaii 96822*
[9]*High Energy Accelerator Research Organization (KEK), Tsukuba*
[10]*Institute of High Energy Physics, Chinese Academy of Sciences, Beijing*
[11]*Institute of High Energy Physics, Vienna*
[12]*Institute of High Energy Physics, Protvino*
[13]*Institute for Theoretical and Experimental Physics, Moscow*
[14]*J. Stefan Institute, Ljubljana*
[15]*Kanagawa University, Yokohama*
[16]*Korea University, Seoul*
[17]*Swiss Federal Institute of Technology of Lausanne, EPFL, Lausanne*
[18]*University of Ljubljana, Ljubljana*
[19]*University of Maribor, Maribor*
[20]*University of Melbourne, Victoria*
[21]*Nagoya University, Nagoya*
[22]*Nara Women's University, Nara*
[23]*National Central University, Chung-li*
[24]*National United University, Miao Li*
[25]*Department of Physics, National Taiwan University, Taipei*
[26]*H. Niewodniczanski Institute of Nuclear Physics, Krakow*
[27]*Nippon Dental University, Niigata*
[28]*Niigata University, Niigata*
[29]*University of Nova Gorica, Nova Gorica*
[30]*Osaka City University, Osaka*
[31]*Osaka University, Osaka*

[32]Panjab University, Chandigarh
[33]Peking University, Beijing
[34]Princeton University, Princeton, New Jersey 08544
[35]RIKEN BNL Research Center, Upton, New York 11973
[36]Saga University, Saga
[37]University of Science and Technology of China, Hefei
[38]Seoul National University, Seoul
[39]Shinshu University, Nagano
[40]Sungkyunkwan University, Suwon
[41]University of Sydney, Sydney, New South Wales
[42]Toho University, Funabashi
[43]Tohoku Gakuin University, Tagajo
[44]Tohoku University, Sendai
[45]Department of Physics, University of Tokyo, Tokyo
[46]Tokyo Institute of Technology, Tokyo
[47]Tokyo Metropolitan University, Tokyo
[48]Tokyo University of Agriculture and Technology, Tokyo
[49]Virginia Polytechnic Institute and State University, Blacksburg, Virginia 24061
[50]Yonsei University, Seoul
[51]University of Melbourne, School of Physics, Victoria 3010
(Received 21 March 2007; published 18 September 2007)

We report measurements of branching fractions for $B \to K\pi$ and $B \to \pi\pi$ decays based on a data sample of 449×10^6 $B\bar{B}$ pairs collected at the $\Upsilon(4S)$ resonance with the Belle detector at the KEKB asymmetric-energy e^+e^- collider. We also measure the ratios of partial widths for $B \to K\pi$ decays, namely $R_c \equiv 2\Gamma(B^+ \to K^+\pi^0)/\Gamma(B^+ \to K^0\pi^+) = 1.08 \pm 0.06 \pm 0.08$ and $R_n \equiv \Gamma(B^0 \to K^+\pi^-)/2\Gamma(B^0 \to K^0\pi^0) = 1.08 \pm 0.08 \pm 0.08$, where the first and the second errors are statistical and systematic, respectively. These ratios are sensitive to enhanced electroweak penguin contributions from new physics; the new measurements are, however, consistent with standard model expectations.

DOI: 10.1103/PhysRevLett.99.121601 PACS numbers: 13.25.Hw, 11.30.Er, 12.15.Hh, 14.40.Nd

Tests of the standard model (SM) can be performed in B-meson decays to $K\pi$ and $\pi\pi$ final states, which involve various interplays between dominant $b \to u$ tree diagram, $b \to s, d$ penguin diagrams and other subdominant contributions. In general, direct comparisons of the measured branching fractions with SM predictions suffer from large hadronic uncertainties within the current theoretical framework. However, many of the uncertainties cancel out in ratios of branching fractions. Previous experimental results [1–3] for the ratios $R_c \equiv 2\Gamma(B^+ \to K^+\pi^0)/\Gamma(B^+ \to K^0\pi^+) = 1.00 \pm 0.08$ and $R_n \equiv \Gamma(B^0 \to K^+\pi^-)/2\Gamma(B^0 \to K^0\pi^0) = 0.82 \pm 0.08$ [4] deviate from SM expectations, calculated within several approaches [5–9]. For example, Ref. [6] predicts the values $R_c = 1.15 \pm 0.05$ and $R_n = 1.12 \pm 0.05$, which are calculated assuming $SU(3)$ flavor symmetry. If the differences between these SM expectations and the measured values of R_c and R_n persist with more data, this would imply a large electroweak penguin contribution in $B \to K\pi$ decays [6,8,9].

In this Letter, we report new measurements of the branching fractions for $B \to K^+\pi^-$, $K^+\pi^0$, $K^0\pi^0$, $\pi^+\pi^-$ and $\pi^+\pi^0$ decays with a data sample 5 times larger than that used in our previous study [1]. Recent Belle results for $B \to K\bar{K}$, $B^+ \to K^0\pi^+$, and $B^0 \to \pi^0\pi^0$ decays have been reported elsewhere [10,11]. The results are based on a sample of $(449.3 \pm 5.7) \times 10^6 B\bar{B}$ pairs collected with the Belle detector [12] at the KEKB e^+e^- asymmetric-energy (3.5 on 8 GeV) collider [13]. For the first sample of 152×10^6 $B\bar{B}$ pairs (data set I), a 2.0 cm radius beam pipe and a three-layer silicon vertex detector were used; for the latter 297×10^6 $B\bar{B}$ pairs (data set II), a 1.5 cm radius beam pipe, a four-layer silicon detector and a small-cell inner drift chamber were used [14]. The production rates of B^+B^- and $B^0\bar{B}^0$ pairs are assumed to be equal. The inclusion of the charge-conjugate decay is implied, unless explicitly stated otherwise.

Kaons and pions are identified from well-measured charged tracks using a K-π likelihood ratio $\mathcal{R}(K/\pi) = \mathcal{L}_K/(\mathcal{L}_K + \mathcal{L}_\pi)$, where $\mathcal{L}_K$ ($\mathcal{L}_\pi$) is the likelihood that the track is a kaon (pion). Charged tracks with $\mathcal{R}(K/\pi) > 0.6$ (<0.4) are classified as kaons (pions). With a sample of $D^{*+} \to D^0\pi^+$ ($D^0 \to K^-\pi^+$) decays we determine that the $\mathcal{R}(K/\pi)$ requirement typically results in a kaon (pion) identification efficiency of 83% (90%), while 6% (12%) of selected kaons (pions) are misidentified as pions (kaons). Furthermore, we reject charged tracks that are consistent with an electron hypothesis. Candidate K^0 mesons are reconstructed as $K^0_S \to \pi^+\pi^-$ decays [10]. The intersection point of the $\pi^+\pi^-$ pair must be displaced from the interaction point [15]. Pairs of photons with invariant masses in the range of $115\ \mathrm{MeV}/c^2 < M_{\gamma\gamma} < 152\ \mathrm{MeV}/c^2$ ($\pm 3\sigma$) are considered as π^0 candidates.

The photon energy is required to be greater than 50 (100) MeV in the barrel (end-cap) regions of the electromagnetic calorimeter.

Charged and neutral K/π candidates are combined in appropriate pairs to form candidate B mesons. These are identified by the "beam-energy-constrained" mass, $M_{\rm bc} \equiv \sqrt{E^{*2}_{\rm beam}/c^4 - p^{*2}_B/c^2}$, and the energy difference, $\Delta E \equiv E^*_B - E^*_{\rm beam}$, where $E^*_{\rm beam}$ is the run-dependent beam energy, and E^*_B and p^*_B are the reconstructed energy and momentum of the B candidates in the center-of-mass (c.m.) frame, respectively. Events with $M_{\rm bc} > 5.20\ {\rm GeV}/c^2$ and $|\Delta E| < 0.3$ GeV are selected for analysis.

The dominant background is from $e^+e^- \to q\bar{q} (q = u, d, s, c)$ continuum events. We use event topology to distinguish the $B\bar{B}$ events from the jetlike continuum background. Suppression of the continuum is achieved by applying a requirement on the ratio $\mathcal{R} = \mathcal{L}_{\rm sig}/(\mathcal{L}_{\rm sig} + \mathcal{L}_{q\bar{q}})$, where $\mathcal{L}_{\rm sig}$ ($\mathcal{L}_{q\bar{q}}$) is the signal (continuum) likelihood, based on a Monte Carlo (MC) simulation [10]. Continuum background is further suppressed through use of the B-flavor tagging algorithm [16], which provides a discrete variable indicating the flavor of the tagging B meson and a continuous quality parameter r ranging from 0 to 1. We classify events separately as poorly-tagged ($r \le 0.5$) and well-tagged ($r > 0.5$) in data set I and data set II; for each category we determine a continuum suppression requirement for $\mathcal{R}$ that maximizes the value of $N^{\rm exp}_{\rm sig}/\sqrt{N^{\rm exp}_{\rm sig} + N^{\rm exp}_{q\bar{q}}}$. Here, $N^{\rm exp}_{\rm sig}$ denotes the expected signal yields based on MC simulation and the average branching fractions of the previous measurements [1–3], and $N^{\rm exp}_{q\bar{q}}$ denotes the expected continuum yields as estimated from sideband data ($M_{\rm bc} < 5.26\ {\rm GeV}/c^2$ and $|\Delta E| < 0.3$ GeV).

Background contributions from $\Upsilon(4S) \to B\bar{B}$ events are investigated using a large MC sample that includes events from $b \to c$ transitions and charmless B decays, corresponding, respectively, to 3 and 50 times the size of the measured data. After all the selection requirements, no $b \to c$ background is found, while a small contribution from charmless B decays is present at low ΔE values for all studied modes. Because of $K - \pi$ misidentification, large $B^0 \to K^+\pi^-$ and $B^+ \to K^+\pi^0$ feed-across backgrounds appear in the $B^0 \to \pi^+\pi^-$ and $B^+ \to \pi^+\pi^0$ modes, respectively.

The signal yields are extracted by performing extended unbinned maximum likelihood fits to the ($M_{\rm bc}$, ΔE) distributions of the selected candidate events. The likelihood function for each mode is defined as

$$\mathcal{L} = \frac{\exp(-\sum_{l,k,j} N_{l,k,j})}{N!} \prod_i \left(\sum_{l,k,j} N_{l,k,j} P^i_{l,k,j} \right), \qquad (1)$$

where N is the total number of events, i is the event identifier, l indicates data set I or data set II, k distinguishes the two r regions and j runs over all components included in the fitting function: signal, continuum background, feed-across, and charmless B background. The variable $N_{l,k,j}$ denotes the number of events, and $P^i_{l,k,j} = \mathcal{P}_{l,k,j}(M^i_{\rm bc}, \Delta E^i)$ are two-dimensional PDFs, which are the same in the two r regions for all fit components except for the continuum background.

All the signal PDFs ($P_{l,k,j={\rm signal}}(M_{\rm bc}, \Delta E)$) are parameterized by smoothed two-dimensional histograms obtained from correctly reconstructed signal MC events based on the data set I and data set II detector configurations. Signal MC events are generated with the PHOTOS [17] simulation package to take into account final-state radiation. Since the $M_{\rm bc}$ signal distribution is dominated by the beam-energy spread, we use the signal-peak positions and resolutions obtained from $B^+ \to \bar{D}^0\pi^+$ data to refine our signal MC events (the $\bar{D}^0 \to K^+\pi^-\pi^0$ subdecay is used for modes

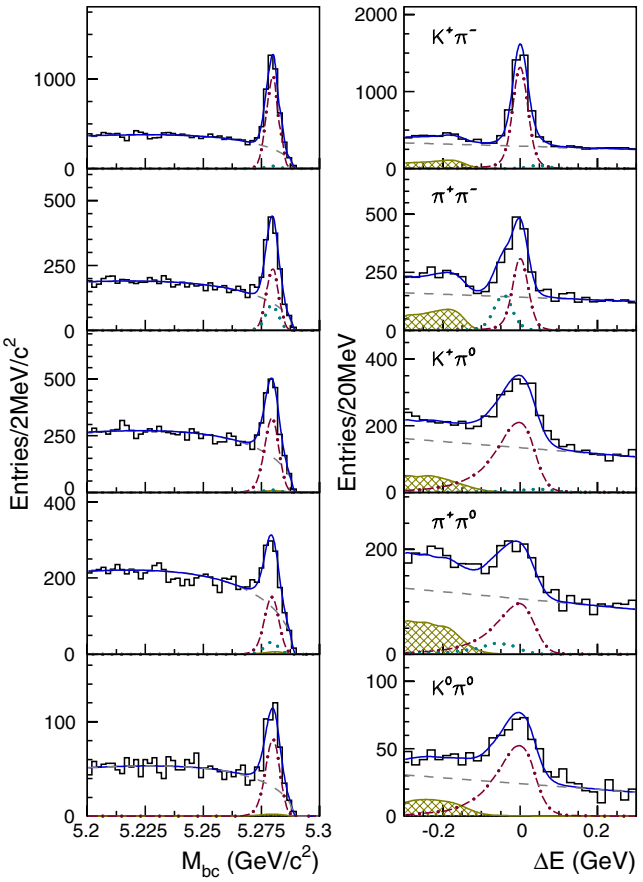

FIG. 1 (color online). $M_{\rm bc}$ (left) and ΔE (right) distributions for $B^0 \to K^+\pi^-$, $B^0 \to \pi^+\pi^-$, $B^+ \to K^+\pi^0$, $B^+ \to \pi^+\pi^0$ and $B^0 \to K^0\pi^0$ candidates. The histograms show the data, while the curves represent the various components from the fit: signal (dot-dashed line), continuum (dashed line), charmless B decays (hatched line), background from misidentification (dotted line), and sum of all components (solid line). The $M_{\rm bc}$ and ΔE projections of the fits are for events that have $|\Delta E| < 0.06$ GeV (left) and $5.271\ {\rm GeV}/c^2 < M_{\rm bc} < 5.289\ {\rm GeV}/c^2$ (right). (A looser requirement, $-0.14\ {\rm GeV} < \Delta E < 0.06$ GeV, is used for the modes with a π^0 meson in the final state).

with a π^0 in the final state, while $\bar{D}^0 \to K^+\pi^-$ is used for the other modes). The resolution for the ΔE distribution is calibrated using the invariant mass distribution of high momentum ($p_{\rm Lab} > 3$ GeV/c) D mesons.

Since the correlation between $M_{\rm bc}$ and ΔE for the continuum background is found to be negligible, the continuum background PDF is described by a product of a linear function for ΔE and an ARGUS function, $f(x) = x\sqrt{1-x^2}\exp[-\xi(1-x^2)]$, where $x = M_{\rm bc}c^2/E^*_{\rm beam}$ [18]. The overall normalization, ΔE slope and ARGUS parameter ξ are free parameters in the fit. The background PDFs for charmless B decays are modeled by a smoothed two-dimensional histogram, obtained from a large MC sample. We also use a smoothed two-dimensional histogram to describe the feed-across background, since the background events have ($M_{\rm bc}$, ΔE) shapes similar to the signal, except for a ΔE peak position shift of $\simeq 45$ MeV. We perform a simultaneous fit for $B^0 \to K^+\pi^-$ and $B^0 \to \pi^+\pi^-$, since these two decay modes feed across into each other. The feed-across fractions are constrained according to the identification efficiencies and fake rates of kaons and pions. A simultaneous fit is also used for the $B^+ \to K^+\pi^0$ and $B^+ \to \pi^+\pi^0$ decay modes.

When likelihood fits are performed, the yields are allowed to float independently for each l (data set I or data set II) and k bin (low or high r region). The $M_{\rm bc}$ and ΔE projections of the fits are shown in Fig. 1, while Table I summarizes the fit results for each mode. The branching fraction of each mode is calculated by dividing the total signal yield by the number of $B\bar{B}$ pairs and by the average reconstruction efficiency. The calculation of the average efficiency takes into account the differences between various l and k bins, and includes branching fractions for $\pi^0 \to \gamma\gamma$ and $K^0 \to K^0_S$ ($K^0_S \to \pi^+\pi^-$) [19].

The fitting systematic errors include the signal PDF modeling, the modeling of the charmless B background, and feed-across constraints. We estimate the first of these errors from the fit deviations after varying the mean and width in $M_{\rm bc}$ and ΔE of the signal PDFs by 1 standard deviation in the calibration factors. The last of the fitting errors is estimated from the fit variations after varying the yields of the feed-across backgrounds by 1 standard deviation. The effects due to fake-rate uncertainties are also included in the systematic error of the feed-across backgrounds. The systematic error due to the charmless B background modeling is evaluated with different PDFs obtained by varying the fractions of the dominant charmless B decay modes within their branching-fraction uncertainties. The above deviations in the signal yield are added in quadrature to obtain the overall systematic error due to fitting.

The MC-data efficiency difference due to the requirement on the likelihood ratio $\mathcal{R}$ is investigated with $B^+ \to \bar{D}^0\pi^+$ samples. The systematic error due to the charged-track reconstruction efficiency is estimated to be 1% per track using partially reconstructed D^* events [20]. The systematic error due to the $\mathcal{R}(K/\pi)$ selection is 1.3% for pions and 1.5% for kaons, respectively. The K^0_S reconstruction efficiency and the associated systematic error are verified by comparing the measured value of the ratio of $D^+ \to K^0_S\pi^+$ and $D^+ \to K^-\pi^+\pi^+$ yields of data set I and data set II with the MC expectations for the control samples, in which we require that the K^0_S momentum be greater than 1.5 GeV/c in order to mimic the high momentum K^0_S in signal decays. Similarly, the π^0 reconstruction efficiency and the systematic error are verified by comparing the ratio of $\bar{D}^0 \to K^+\pi^-$ and $\bar{D}^0 \to K^+\pi^-\pi^0$ yields with the MC expectations, using decays with π^0's selected in a momentum region corresponding to signal decays. For the ratio of the D^+ ($\bar{D}^0$) subdecays branching fractions mentioned above, the difference between the branching fractions used in MC calculations and recent measurements [21] is also taken into account to obtain the correction factor and total systematic uncertainty for the K^0_S (π^0) reconstruction efficiency. Possible systematic uncertainties due to the description of final-state radiation have been studied by comparing the latest theoretical calculations with the PHOTOS MC program [22]. These uncertainties were found to be negligible and thus no systematic error is assigned due to PHOTOS. The systematic error due to the uncertainty of the total number of $B\bar{B}$ pairs is 1.3% and the error due to signal MC statistics is between 0.4% and 0.7%. The final systematic uncertainty is ob-

TABLE I. Extracted signal yields, product of efficiencies, and subdecay branching ratios ($\mathcal{B}_s$), and calculated branching fractions for individual modes. The branching-fraction errors are statistical and systematic, respectively.

Mode	Yield	Eff. $\times$ $\mathcal{B}_s$(%)	$\mathcal{B}(10^{-6})$
$K^+\pi^-$	3585^{+69}_{-68}	40.16	$19.9 \pm 0.4 \pm 0.8$
$\pi^+\pi^-$	872^{+41}_{-40}	37.98	$5.1 \pm 0.2 \pm 0.2$
$K^+\pi^0$	1493^{+57}_{-55}	26.86	$12.4 \pm 0.5 \pm 0.6$
$\pi^+\pi^0$	693^{+46}_{-43}	23.63	$6.5 \pm 0.4 \pm 0.4$
$K^0\pi^0$	379^{+28}_{-27}	9.17	$9.2 \pm 0.7 \pm 0.6$

TABLE II. Summary of systematic errors, given in percent.

	$K^+\pi^-$	$\pi^+\pi^-$	$K^+\pi^0$	$\pi^+\pi^0$	$K^0\pi^0$
Signal PDF	0.2	0.3	0.4	0.5	0.4
Charmless B background	0.1	0.3	0.4	0.4	0.1
Feed-across background	0.4	2.2	0.7	2.5	0.0
$\mathcal{R}$ requirement	1.0	1.0	1.3	1.4	1.5
Tracking	2.0	2.0	1.0	1.0	0.0
$\mathcal{R}(K/\pi)$ requirement	2.9	2.8	1.5	1.3	0.0
K^0_S reconstruction	0.0	0.0	0.0	0.0	4.9
π^0 reconstruction	0.0	0.0	4.0	4.0	4.0
# of $B\bar{B}$	1.3	1.3	1.3	1.3	1.3
Signal MC statistics	0.6	0.4	0.4	0.5	0.7
Total	4.0	4.4	4.9	5.4	6.7

TABLE III. Partial width ratios of $B \to K\pi$ and $\pi\pi$ decays. The errors are quoted in the same manner as in Table I.

Modes	Ratio
$2\Gamma(K^+\pi^0)/\Gamma(K^0\pi^+)$	$1.08 \pm 0.06 \pm 0.08$
$\Gamma(K^+\pi^-)/2\Gamma(K^0\pi^0)$	$1.08 \pm 0.08 \pm 0.08$
$\Gamma(K^+\pi^-)/\Gamma(K^0\pi^+)$	$0.94 \pm 0.04 \pm 0.05$
$\Gamma(\pi^+\pi^-)/\Gamma(K^+\pi^-)$	$0.26 \pm 0.01 \pm 0.01$
$\Gamma(\pi^+\pi^-)/2\Gamma(\pi^+\pi^0)$	$0.42 \pm 0.03 \pm 0.02$
$\Gamma(\pi^+\pi^0)/\Gamma(K^0\pi^0)$	$0.66 \pm 0.07 \pm 0.04$
$2\Gamma(\pi^+\pi^0)/\Gamma(K^0\pi^+)$	$0.57 \pm 0.04 \pm 0.04$

tained by quadratically summing all the contributions, as shown in Table II.

The ratios of partial widths can be used to extract the angle ϕ_3 and to search for new physics [6,8,9]. These ratios (listed in Table III) are obtained from the five measurements in Table I and the new measurement of $\mathcal{B}(B^+ \to K^0\pi^+) = (22.8^{+0.8}_{-0.7} \pm 1.3) \times 10^{-6}$ described in Ref. [10]. The ratio of charged to neutral B meson lifetime, $\tau_{B^+}/\tau_{B^0} = 1.076 \pm 0.008$ [4], is used to convert the branching-fraction ratios into the ratios of partial widths. The total errors are reduced because of the cancellation of some common systematic errors. With a factor of 5 times more data than that used for our previous published results [1], the statistical errors on the branching fractions for all decay modes are reduced by more than a factor of 2.3. The central value of the $K^0\pi^0$ branching fraction has decreased from 11.7×10^{-6} to 9.2×10^{-6} and the $K^+\pi^-$ branching fraction has increased from 18.5×10^{-6} to 19.9×10^{-6}, resulting in a change in R_n from 0.79 ± 0.18 to 1.08 ± 0.12. The obtained value of $R_c = 1.08 \pm 0.10$ is similar to the previous Belle measurement (1.09 ± 0.19) but is more precise. The errors for R_n and R_c shown here are the sum in quadrature of the statistical and systematic errors. These two ratios are now consistent with SM expectations [6–9]. Consequently, the most recent world average values, $R_c = 1.11 \pm 0.07$ and $R_n = 0.99 \pm 0.07$ [23], also show the same tendency.

In conclusion, we have measured the branching fractions for $B \to K\pi$ and $B \to \pi\pi$ decays with 449×10^6 $B\bar{B}$ pairs collected at the $\Upsilon(4S)$ resonance with the Belle detector. We confirm the expected hierarchy of branching fractions: $\mathcal{B}(K^0\pi^+) \geq \mathcal{B}(K^+\pi^-) > \mathcal{B}(K^+\pi^0) \geq \mathcal{B}(K^0\pi^0) > \mathcal{B}(\pi^+\pi^0) \geq \mathcal{B}(\pi^+\pi^-)$ [5,7] and find no significant deviation from SM expectations in the ratios of partial widths. The ratios R_n and R_c are both in good agreement with SM expectations, in contrast to early measurements [1–3].

We thank the KEKB group for excellent operation of the accelerator, the KEK cryogenics group for efficient solenoid operations, and the KEK computer group and the NII for valuable computing and Super-SINET network support. We acknowledge support from MEXT and JSPS (Japan); ARC and DEST (Australia); NSFC and KIP of CAS (China); DST (India); MOEHRD, KOSEF and KRF (Korea); KBN (Poland); MIST (Russia); ARRS (Slovenia); SNSF (Switzerland); NSC and MOE (Taiwan); and DOE (USA).

[1] Y. Chao *et al.* (Belle Collaboration), Phys. Rev. D **69**, 111102 (2004).
[2] B. Aubert *et al.* (*BABAR* Collaboration), Phys. Rev. D **71**, 111102 (2005); Phys. Rev. Lett. **94**, 181802 (2005); Phys. Rev. Lett. **97**, 171805 (2006); Phys. Rev. D **75**, 012008 (2007).
[3] A. Bornheim *et al.* (CLEO Collaboration), Phys. Rev. D **68**, 052002 (2003).
[4] The average results in Winter 2006 by the HFAG group.
[5] M. Beneke, G. Buchalla, M. Neubert, and C. T. Sachrajda, Nucl. Phys. **B606**, 245 (2001).
[6] A. J. Buras, R. Fleischer, S. Recksiegel, and F. Schwab, Eur. Phys. J. C **45**, 701 (2006).
[7] H.-N. Li, S. Mishima, and A. I. Sanda, Phys. Rev. D **72**, 114005 (2005).
[8] T. Yoshikawa, Phys. Rev. D **68**, 054023 (2003); S. Mishima and T. Yoshikawa, Phys. Rev. D **70**, 094024 (2004).
[9] M. Gronau and J. L. Rosner, Phys. Lett. B **572**, 43 (2003).
[10] S.-W. Lin *et al.* (Belle Collaboration), Phys. Rev. Lett. **98**, 181804 (2007).
[11] Y. Chao *et al.* (Belle Collaboration), Phys. Rev. Lett. **94**, 181803 (2005).
[12] A. Abashian *et al.* (Belle Collaboration), Nucl. Instrum. Methods Phys. Res., Sect. A **479**, 117 (2002).
[13] S. Kurokawa and E. Kikutani, Nucl. Instrum. Methods Phys. Res., Sect. A **499**, 1 (2003), and other papers included in this volume.
[14] Z. Natkaniec *et al.* (Belle SVD2 Group), Nucl. Instrum. Methods Phys. Res., Sect. A **560**, 1 (2006).
[15] The K^0_S selection is described in K. -F. Chen *et al.* (Belle Collaboration), Phys. Rev. D **72**, 012004 (2005).
[16] H. Kakuno *et al.*, Nucl. Instrum. Methods Phys. Res., Sect. A **533**, 516 (2004).
[17] E. Barberio and Z. Was, Comput. Phys. Commun. **79**, 291 (1994); P. Golonka and Z. Was, Eur. Phys. J. C **45**, 97 (2006). We use PHOTOS version 2.13 allowing the emission of up to two photons, with an energy cutoff at 1% of the energy available for photon emission (i.e., approximately 26 MeV for the first emitted photon). PHOTOS also takes into account interference between charged final-state particles.
[18] H. Albrecht *et al.* (ARGUS Collaboration), Phys. Lett. B **241**, 278 (1990).
[19] W.-M. Yao *et al.* (Particle Data Group), J. Phys. G **33**, 1 (2006).
[20] Y.-T. Tsai, P. Chang *et al.* (Belle Collaboration), Phys. Rev. D **75**, 111101(R) (2007).
[21] Q. He *et al.* (CLEO Collaboration), Phys. Rev. Lett. **95**, 121801 (2005).
[22] G. Nanava and Z. Was, Eur. Phys. J. C **51**, 569 (2007).
[23] R. Fleischer, S. Recksiegel, and F. Schwab, Eur. Phys. J. C **51**, 55 (2007).